Monthly Notices of the ROYAL ASTRONOMICAL SOCIETY
MNRAS **517,** 4575–4589 (2022) https://doi.org/10.1093/mnras/stac2258

Galaxy And Mass Assembly: galaxy morphology in the green valley, prominent rings, and looser spiral arms

Dominic Smith,[1★] Lutz Haberzettl,[1] L. E. Porter,[1★] Ren Porter-Temple,[1] Christopher P. A. Henry,[1] Benne Holwerda,[1★] Á. R. López-Sánchez,[2,3,4] Steven Phillipps,[5] Alister W. Graham,[6] Sarah Brough,[7] Kevin A. Pimbblet,[8] Jochen Liske,[9] Lee S. Kelvin,[10] Clayton D. Robertson,[1] Wade Roemer,[1] Michael Walmsley,[11] David O'Ryan[12] and Tobias Géron[13]

[1]*Department of Physics and Astronomy, University of Louisville, Natural Science Building 102, 40292 KY Louisville, USA*
[2]*Australian Astronomical Optics, Macquarie University, 105 Delhi Rd, North Ryde, NSW 2113, Australia*
[3]*Department of Physics and Astronomy, Macquarie University, NSW 2109, Australia*
[4]*ARC Centre of Excellence for All Sky Astrophysics in 3 Dimensions (ASTRO-3D), Australia*
[5]*Astrophysics Group, School of Physics, University of Bristol, Tyndall Avenue, Bristol BS8 1TL, UK*
[6]*Centre for Astrophysics and Supercomputing, Swinburne University of Technology, Hawthorn, VIC 3122, Australia*
[7]*School of Physics, University of New South Wales, NSW 2052, Australia*
[8]*E.A. Milne Centre for Astrophysics, University of Hull, Cottingham Road, Kingston-upon-Hull HU6 7RX, UK*
[9]*Hamburger Sternwarte, Universität Hamburg, Gojenbergsweg 112, D-21029 Hamburg, Germany*
[10]*Department of Astrophysical Sciences, Princeton University, 4 Ivy Lane, Princeton, NJ 08544, USA*
[11]*Jodrell Bank Centre for Astrophysics, Department of Physics & Astronomy, University of Manchester, Oxford Road, Manchester M13 9PL, UK*
[12]*Observational Astrophysics Group, Lancaster University, Lancaster LA1 4YW, UK*
[13]*Department of Physics, University of Oxford, Denys Wilkinson Building, Keble Road, Oxford OX1 3RH, UK*

Accepted 2022 July 28. Received 2022 July 28; in original form 2022 May 19

ABSTRACT

Galaxies fall broadly into two categories: star-forming (blue) galaxies and quiescent (red) galaxies. In between, one finds the less populated 'green valley'. Some of these galaxies are suspected to be in the process of ceasing their star formation through a gradual exhaustion of gas supply, or already dead and experiencing a rejuvenation of star formation through fuel injection. We use the Galaxy And Mass Assembly (GAMA) database and the Galaxy Zoo citizen science morphological estimates to compare the morphology of galaxies in the green valley with those in the red sequence and blue cloud. Our goal is to examine the structural differences within galaxies that fall in the green valley, and what brings them there. Previous results found that disc features such as rings and lenses are more prominently represented in the green-valley population. We revisit this with a similar sized data set of galaxies with morphology labels provided by the Galaxy Zoo for the GAMA fields based on new Kilo-Degree Survey (KiDS) images. Our aim is to compare the results from expert classification qualitatively with those of citizen science. We observe that ring structures are indeed found more commonly in green-valley galaxies compared with their red and blue counterparts. We suggest that ring structures are a consequence of disc galaxies in the green valley actively exhibiting the characteristics of fading discs and evolving disc morphology of galaxies. We note that the progression from blue to red correlates with loosening spiral-arm structure.

Key words: galaxies: bar – galaxies: bulges – galaxies: disc – galaxies: evolution – galaxies: spiral – galaxies: star formation.

1 INTRODUCTION

Previous large-scale surveys of galaxies have revealed a bimodality in the colour–magnitude diagram of galaxies with two distinct populations: one with blue optical colours and another with red optical colours (Strateva et al. 2001; Baldry et al. 2004, 2006; Bell et al. 2004; Willmer et al. 2006; Faber et al. 2007; Martin et al. 2007; Ball, Loveday & Brunner 2008; Brammer et al. 2009; Mendez et al. 2011; Taylor et al. 2015; Corcho-Caballero, Ascasibar & López-Sánchez 2020; Corcho-Caballero et al. 2021). These populations were dubbed the 'blue cloud' (BC) or 'star-forming galaxy sequence' and the 'red sequence' (RS), respectively (Driver et al. 2006; Faber et al. 2007; Salim 2014). The blue cloud and red sequence are best separated at higher stellar mass and mix at lower stellar masses (cf. Taylor et al. 2015).

The Galaxy Zoo (GZ) project (Lintott et al. 2008), which produced morphological classifications for a million galaxies, helped to confirm that this bimodality is not entirely morphology-driven (Salim

★ E-mail: dominic.smith@louisville.edu (DS); lori.porter@louisville.edu (LEP); benne.holwerda@gmail.com (BH)

© 2022 The Author(s)
Published by Oxford University Press on behalf of Royal Astronomical Society

Downloaded from https://academic.oup.com/mnras/article/517/3/4575/6795245 by Lancaster University user on 10 December 2022

et al. 2007; Schawinski et al. 2007; Bamford et al. 2009; Skibba et al. 2009: Fig. 1). It suggested larger fractions of spiral galaxies in the red sequence[1] (Masters et al. 2010) and elliptical galaxies in the blue cloud (Schawinski 2009) than had previously been detected.

The sparsely populated colour–mass space between these two populations, the so-called 'green valley' (Fig. 2), provides clues to the nature and duration of galaxy transitions from blue cloud to red sequence. This transition must occur on rapid time-scales, otherwise there would be an accumulation of galaxies residing in the green valley, rather than an accumulation in the red sequence as is observed (Arnouts et al. 2007; Martin et al. 2007; Smethurst et al. 2015, 2017; Nogueira-Cavalcante et al. 2018; Bremer et al. 2018; Phillipps et al. 2019; Barone et al. 2022). Alternatively, gas infall on to red-sequence galaxies may rejuvenate them into the green valley (e.g. Graham et al. 2017). Green-valley galaxies have therefore long been thought of as the 'crossroads' of galaxy evolution, a transitional population between the two main galactic stages of the star-forming blue cloud and the 'red and dead' sequence (Bell et al. 2004; Faber et al. 2007; Martin et al. 2007; Mendez et al. 2011; Schawinski et al. 2014; Pan et al. 2015; Graham 2019); however, it is possible that these are also red-sequence galaxies that have been rejuvenated (Graham et al. 2015, 2017).

The intermediate colours of these green-valley galaxies have been interpreted as evidence for recent quenching (suppression) of star formation (Salim et al. 2007; Salim 2014; Smethurst et al. 2015; Phillipps et al. 2019). Star-forming galaxies are observed to lie on a well-defined stellar mass–star-formation rate (SFR) relation (Martin et al. 2005); however, quenching a galaxy causes it to depart from this relation (Noeske et al. 2007; Peng et al. 2010). The main mechanism for galaxy quenching is thought to be a lack of fuel for star formation. Fading of the star-forming disc, the primary site of star formation, drives the apparent morphological transition of galaxies from spiral to lenticular or elliptical in those galaxies that are quenching and lie in the green valley (Coenda, Martínez & Muriel 2018; Bluck et al. 2020; Fraser-McKelvie et al. 2019, 2020a,b).

Kelvin et al. (2018) examined 472 galaxies in the Galaxy And Mass Assembly (GAMA) survey with Sloan Digital Sky Survey (SDSS) imaging visually for signs of disc substructures (e.g. rings, bars, and lenses) with a team of expert classifiers. They found evidence that rings and lenses are more common in the green valley than in red-sequence and blue-cloud galaxies. Our goal here is to re-examine this result using the GZ morphological estimates using higher resolution and deeper Kilo-Degree Survey (KiDS) images (Kuijken et al. 2019) of the galaxies in the GAMA survey's equatorial fields (Driver et al. 2011). Our sample is of similar size to that of Kelvin et al. (2018) (396 versus 472) and there is likely overlap. There are two critical differences: the method of classification and the quality of the data. Our classifications are based on much improved data and arrived at with citizen science voting rather than a small expert panel. Our aim is to examine whether the different data and classification schemes arrive at qualitatively the same conclusions for the morphology of the green valley.

Our work is organized as follows: Section 2 describes the GAMA and GZ data we use here, Section 3 presents our results, and we discuss these in Section 4. Section 5 lists our conclusions.

[1]The red sequence was originally known as the colour–magnitude relation for early-type galaxies, see the review in Graham (2013).

2 DATA

In this work, we use GAMA and GZ voting data based on KiDS imaging.

2.1 GAMA

The GAMA survey is a spectroscopic survey comprised of three equatorial fields and two southern fields. Its multi-wavelength photometry ranges from ultraviolet to submm wavelengths (Driver et al. 2009; Hopkins et al. 2013; Liske et al. 2015). Redshifts (z) are found reliably to $z\sim0.8$ and the survey is complete to $\sim$98 per cent for an apparent magnitude in the Sloan Digital Sky Survey r filter (SDSS-r) of 19.8 mag in the equatorial fields. Here, we consider only these (G09, G12, and G15), as they overlap with KiDS (de Jong et al. 2013, 2015, 2017; Kuijken et al. 2019), on which the GZ information is based (see next section).

We use GAMA optical photometry from SDSS Stripe-82 photometry (Taylor et al. 2011), which is corrected for redshift (K correction) and internal dust extinction. The final photometry we used is the Lambda Adaptive Multi-Band Deblending Algorithm in R (LAMBDAR) photometry (v01) presented in Wright et al. (2017).

Separately, we use stellar masses derived from the spectral energy distribution (SED) model fit using the MAGPHYS tool (da Cunha, Charlot & Elbaz 2008), presented in Driver et al. (2016) and Wright et al. (2017) (v06 in DR3).

2.2 KiDS GZ

The GZ citizen science project analysed KiDS (de Jong et al. 2013, 2015, 2017; Kuijken et al. 2019) images. Citizen scientists answered a series of questions based on KiDS g- and r-band imaging. A synthetic green channel was constructed as the arithmetic mean of the other two to allow for the construction of three-colour RGB images. Because morphological detail is lost with distance, a limit of $z \leq 0.075$ is enforced to ensure reliable morphological estimates of kpc-scale structures (e.g. spiral arms, bars). Initially we ran this data with $z \leq 0.15$; however, we realized limitations in the GZ data that limited us to $z \leq 0.08$, making resolution for many morphological structures difficult. Therefore, we decided to restrict our sample to $z \leq 0.075$ to limit the bias due to distance effects in the GZ voting.

The GZ question tree is presented in Holwerda et al. (2019) and in Fig. 1. The full GZ classification is described in Kelvin et al. (in preparation). We focus on the questions that are asked in the GZ question tree (Fig. 1) regarding disc galaxy morphology. In Section 3, we begin each subsection with the question code and associated question for the morphological features as asked in the GZ questionnaire. These question codes are T00, T01, T02, T03, T04, T05, T06, T09, and T10. We refer the reader to Kelvin et al. (in preparation) for specific details of the GZ analysis. We used an internal GAMA/KiDS catalogue for the subsequent analysis.

2.3 Sample selection

We organized our GZ data by stellar mass, $\log(M_*)/\mathrm{M}_\odot$, versus intrinsic stellar population colour plane ($u* - r*$) (the population selections are from Bremer et al. 2018). Fig. 2 shows our selection of blue-cloud, green-valley, and red-sequence galaxies, based on their stellar mass and rest-frame colour. A second requirement is that these galaxies are disc-dominated following the T00 question (Fig. 1): 'Is the galaxy in the centre of the image simply smooth and rounded or does it have features?' with any fraction of the votes in favour of any

Downloaded from https://academic.oup.com/mnras/article/517/3/4575/6795245 by Lancaster University user on 10 December 2022

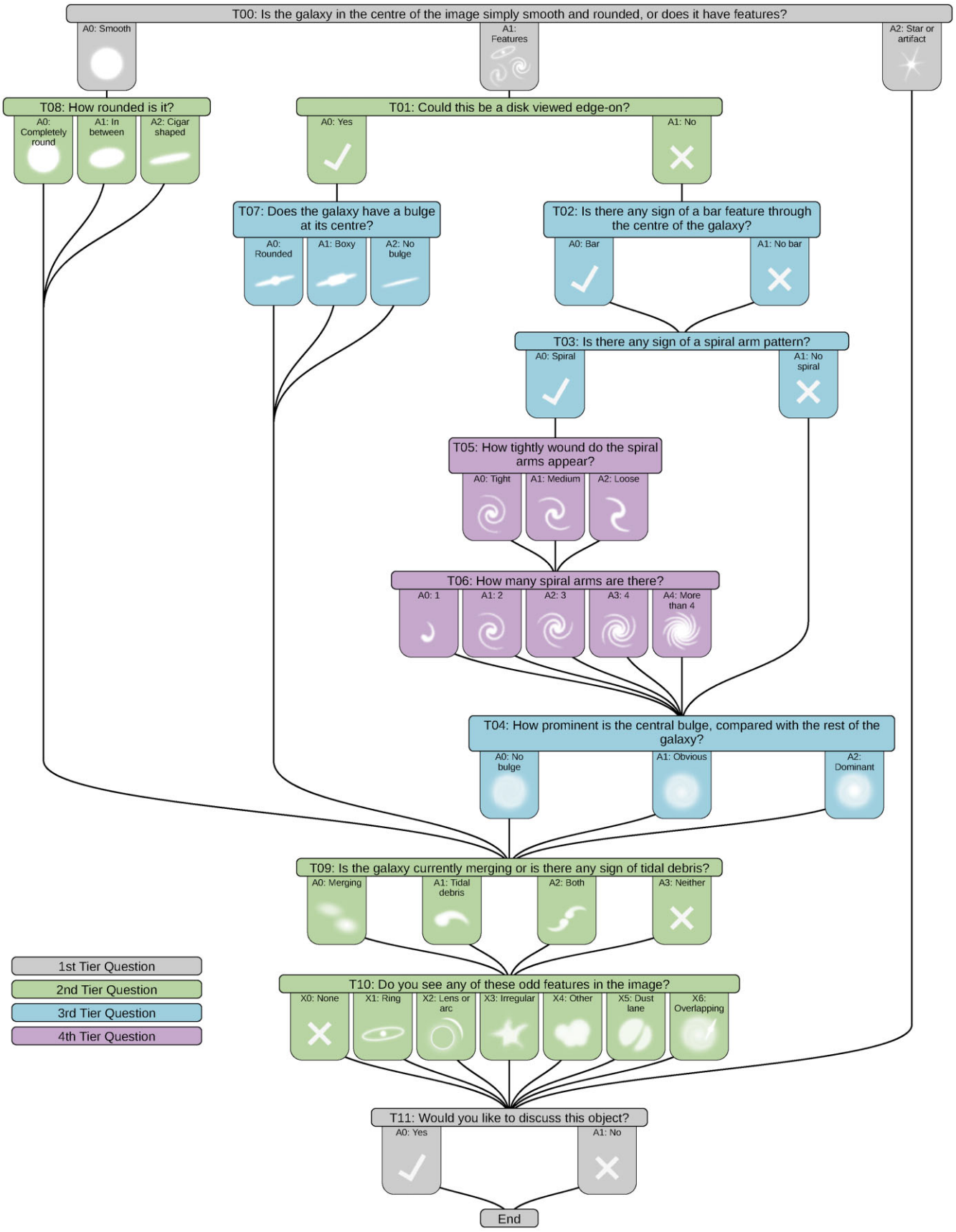

Figure 1. The flow diagram of the GZ4 (fourth generation) question tree. We refer to the text for details on the questions in the GAMA sample.

Downloaded from https://academic.oup.com/mnras/article/517/3/4575/6795245 by Lancaster University user on 10 December 2022

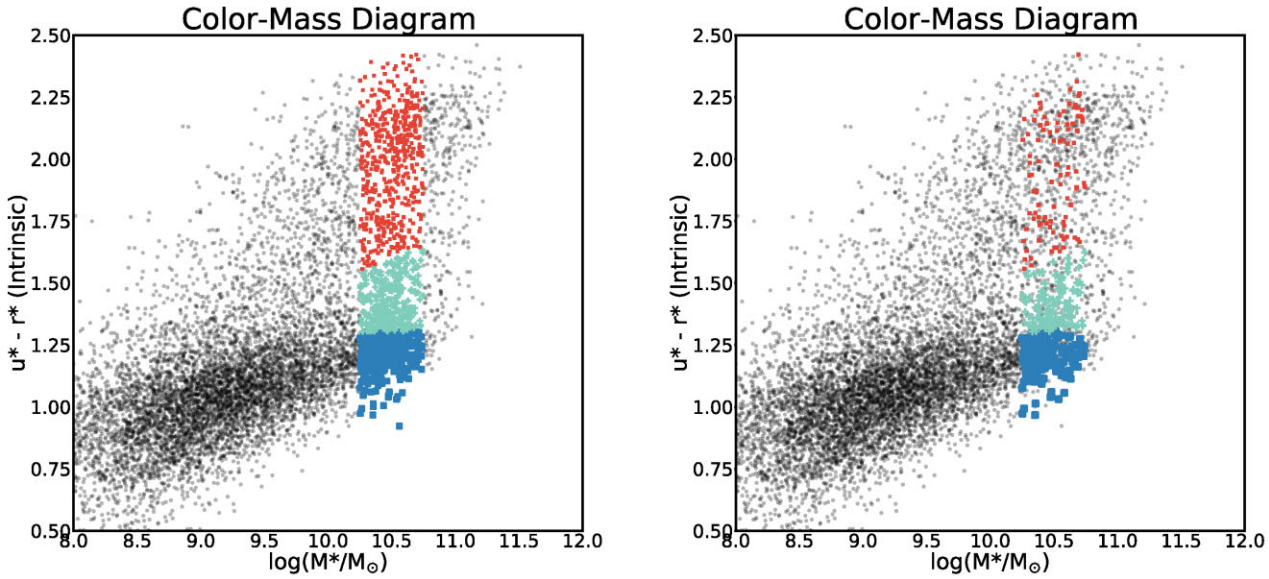

Figure 2. These plots represent all the GAMA galaxies in our mass range ($10.25 < \log(M_*/\mathrm{M}_\odot) < 10.75$), colour-coded for their classification. We use the limits from Bremer et al. (2018) to select red, green, and blue galaxies. The left panel represents all the respective galaxies in their mass ranges before further data selection. The right panel shows all galaxies with any votes between 0.1 and 1 for not being seen edge-on and votes between 0.3 and 1 for spiral features. The right image represents our current data selection.

features ($f_{\mathrm{features}} > 0$). This is to remove any galaxies without features to examine further.

For the first graph in Fig. 2, we limited the mass to $10.25 < \log(M_*/\mathrm{M}_\odot) < 10.75$ and the redshift to $z \leq 0.075$. This mass range was selected to ensure a complete sample and for more direct comparison with Kelvin et al. (2018), who select galaxies in the same mass range. This mass range covers the tip of the blue cloud at low z; this is necessary because, for galaxies to continue evolving beyond this point, they must transition across the green valley (Bremer et al. 2018). The redshift limit was imposed to ensure that distance effects on the GZ voting are minimal (see the discussion in Willett et al. 2013 on distance effects). Beyond $z = 0.075$, the resolution of KiDS images is not sufficient to discriminate between features a kiloparsec in size, such as the width of spiral arms and rings. The voting can be corrected using debiasing, but the GAMA dataset may be too small for this (however, Galaxy Zoo v4 will be).

The right graph of Fig. 2 represents the galaxies in each faction that, in GZ, have any votes for 'Could this be a disc viewed edge on?' as no and 'Is there any sign of a spiral arm pattern?' registering 30 per cent or higher (T01 and T03 in Fig. 1, respectively). To do this, we set the voting for T01 results to fraction limits between 0.0001 and 0.9999 to prevent the possible error of galaxies with single votes throwing off the results, and to maximize those votes for features. We continued to do the same with T02; however, this time we set the limits between 0.3 and 1. This allowed us to choose galaxies that had votes for bulges, spiral features, and all other morphological features in this branch of the questionnaire. Lastly, for this step we limited our selection for spiral features in the same way. We were left with a data set of 176 for the blue cloud, 118 for the green valley, and 102 for the red sequence, giving a total of 396 galaxies in the mass range considered.

Fig. 3 shows the distribution of featured galaxies in redshift (z) and stellar mass (M_*). Our selection is made to the specifications $10.25 < \log(M_*/\mathrm{M}_\odot) < 10.75$ and $z \leq 0.075$, the redshift limit of GZ pre-selection for classification. This gives us a good representative

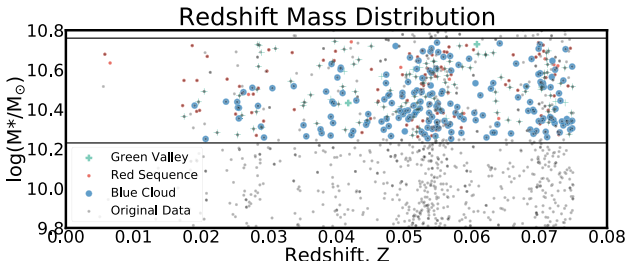

Figure 3. A scatter plot of the blue, green, and red galaxies in our sample extracted from GAMA to compare with GZ voting. The coloured galaxies represent the 396 galaxies that composed our selected sample, represented by the right panel of Fig. 2. The GAMA sample is taken for $10.25 < \log(M_*/\mathrm{M}_\odot) < 10.75$ at $z \leq 0.075$, which is the redshift limit of the GZ selection from KiDS. The colour criteria are from Bremer et al. (2018).

volume to compare galaxy morphologies. We find that red-sequence galaxies are at slightly higher masses than the blue cloud, with green-valley galaxies spanning an intermediate mass range. The galaxy spread is represented better by mass in Fig. 4.

3 RESULTS

We compared the normalized fractions of galaxies between blue-cloud, green-valley, and red-sequence galaxies to generate voting histograms and violin plots showing sample fractions in the following subsections.

As shown in Fig. 1, each tier was signified with a code, T##. This code represents the question asked in GZ about a morphological trait, with the number denoting the tier of each question. We organized each subsection by these question codes with their data represented in a histogram.

The tool used to compare these data is the Kolmogorov–Smirnov (K–S) two-sample similarity test and the associated p-value calculated for our selection samples. The K–S value provides the

Downloaded from https://academic.oup.com/mnras/article/517/3/4575/6795245 by Lancaster University user on 10 December 2022

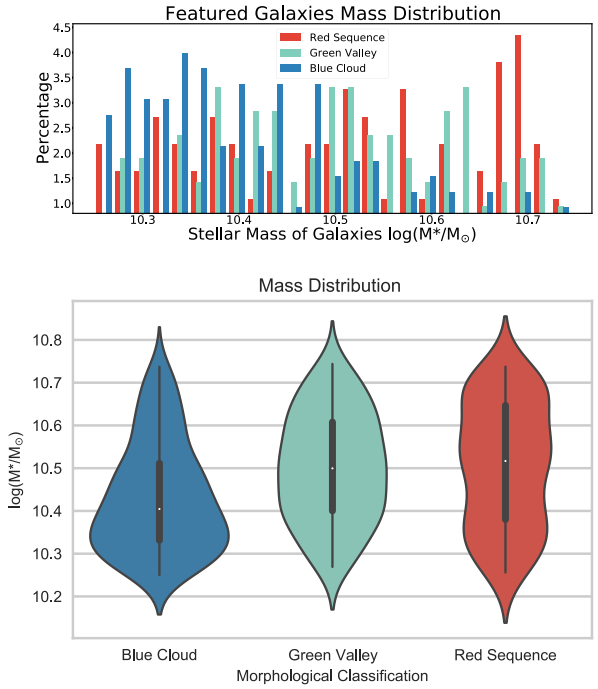

Figure 4. A histogram of the blue, green, and red galaxies in our selection sample (right panel of Fig. 2) extracted from GAMA to compare with GZ voting. The GAMA sample is taken for $(10.25 < \log(M_*/M_\odot) < 10.75)$ and $z \leq 0.15$, the limit of the GZ selection from KiDS. The histogram illuminates the overlap of data presented in Fig. 3. The violin plot below shows the same information as the histogram above it.

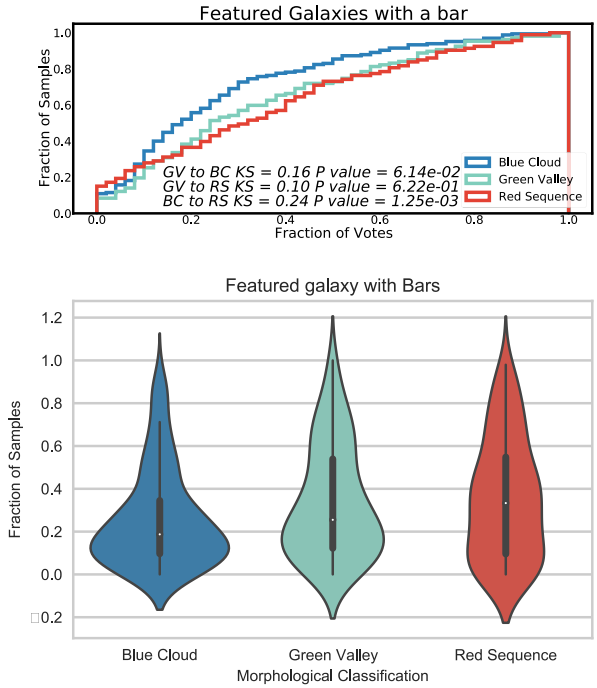

Figure 5. A histogram of the fraction of votes in favour of classifying galaxies as featured with a bar (T02 in the GZ questionnaire). The difference between the three groups is nearly equally distinguishable, with K–S values of 0.16 for green valley and blue cloud, 0.10 for green valley and red sequence, and 0.24 for blue cloud and red sequence. The significance from p-values is 6.14×10^{-02}, 6.22×10^{-01}, and 1.25×10^{-03}, respectively. This confirms that the three groups are statistically variant. The violin plots represent the same data.

maximum difference between any two cumulative distributions we consider. The p-value is the probability of random occurrence of the presented null hypothesis (the distributions are the same).

We plot the voting in GZ in two ways in each of the following figures. In the upper panel, we plot the cumulative histogram of the voting in GZ: on the x-axis is the fraction of voting in favour of the question under consideration and on the y-axis the fraction of the sample is shown. A plot that rises early has a larger fraction of the sample with a low fraction of the votes in favour of this feature being present. In this case, the feature is relatively rare. If the plot rises on the right of the x-axis, a large fraction of the sample has a high fraction of votes (or greater consensus) that this feature is present.

In the lower panel, we present the same fraction of the voting in a more traditional histogram, rendered as a violin plot (a mirrored histogram with a kernel density applied to render it into a smooth graph). Because the distribution is slightly smoothed, the range of values on the y-axes in the figures goes from -0.2 to 1.2 to accommodate the tails resulting from kernel smoothing. The range and standard deviation of the distribution are also shown as thin and thick horizontal lines.

By combining both graphical visualizations in each plot, we hope to show both when voting behaviour between populations is similar or dissimilar in the cumulative distribution, reflected in the K–S metric, and how the voting behaviour looks in each population in a more intuitive histogram rendering.

3.1 Bars

Fig. 1, T02: *'Is there a sign of a bar feature through the centre of the galaxy?'*

Stellar bars are a prime suspect for a morphological feature that aids in quenching, especially quenching from the inside out (see Masters et al. 2021 for a review).

GZ voting shows that the red sequence and green valley have a lower fraction of galaxies having bar-shaped structures than the blue cloud. In our statistical analysis, we have chosen only to include galaxies that were voted as bar galaxies 50 per cent ($f_{\rm bar}$ > 0.5) or more of the time. From our galaxy sample for each faction, 12.1 per cent of blue-cloud, 20.1 per cent of green-valley, and 19.3 per cent of red-sequence galaxies met this requirement. These percentages are to be expected if the green valley is a transition zone and bars are in fact a predecessor to quenching and are long-lived enough to do so. Fig. 5 shows similar voting behaviour in GZ in the red sequence and green valley. The notably different behaviour in the blue cloud shows lower confidence in more of the blue-cloud sample of galaxies.

3.2 Featured discs

Fig. 1, T03: *'Is there any sign of a spiral arm pattern?'*

Using the voting data from this question showed galaxies with spiral features in the red sequence, blue cloud, and green valley.

The outcome, as shown in Fig. 6, shows that most disc galaxies in the blue cloud are featured galaxies. There are fewer featured galaxies among the disc galaxies of the red sequence. The number of featured galaxies in the green valley falls somewhere in between those present in the blue cloud and red sequence. The fraction of galaxies with discs

Downloaded from https://academic.oup.com/mnras/article/517/3/4575/6795245 by Lancaster University user on 10 December 2022

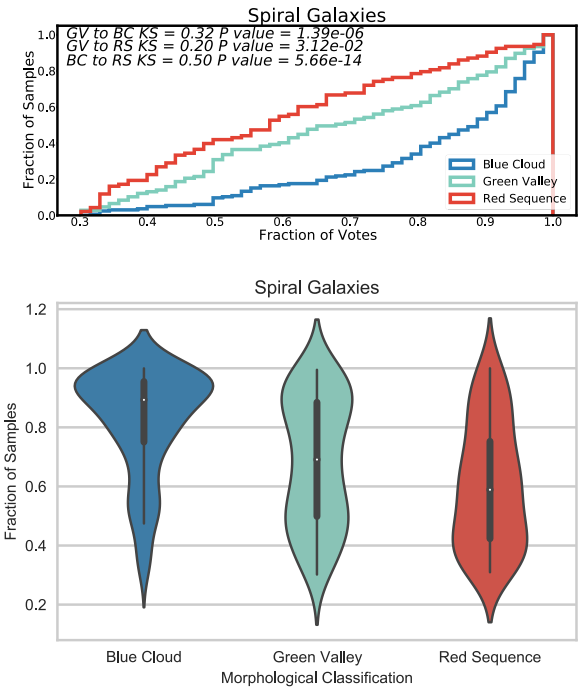

Figure 6. A histogram of the fraction of votes in favour of classifying galaxies as featured (T00 in the GZ questionnaire). According to the K–S test, the green valley and blue cloud are very distinguishable, with a value of 0.37. The difference between the green valley and red sequence is distinguishable as well, with a KS value of 0.20. The difference between the blue cloud and red sequence yields a KS value of 0.50. These differences are confirmed further due to very small p-values: 1.39×10^{-06}, 3.12×10^{-02}, and 5.66×10^{-14}, respectively. The violin plots represent the same data as the cumulative histogram at the top.

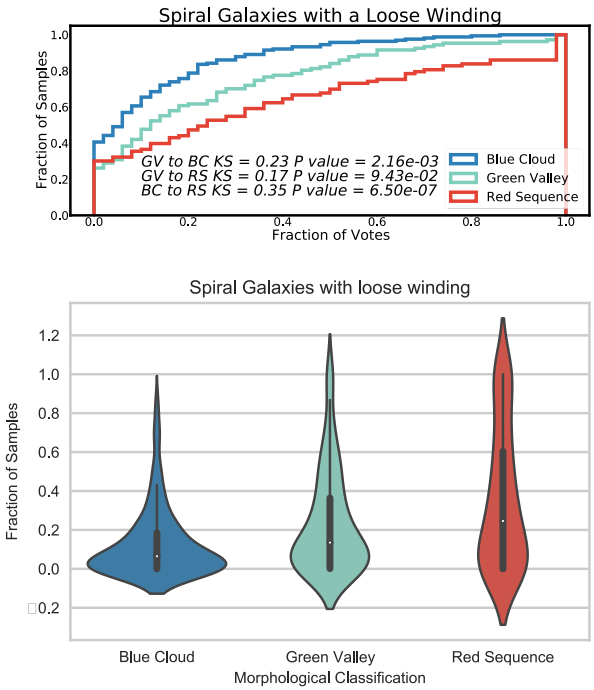

Figure 7. Histogram of the fraction of votes in favour of spiral galaxies having a loose winding (T05 in the GZ questionnaire). The difference between green-valley and blue-cloud galaxies is distinguishable with a KS of 0.23, the KS of green-valley and red-sequence galaxies is 0.17, and the KS of the blue cloud and red sequence is 0.35. Green valley to blue cloud has a p value of 2.16×10^{-03}, green valley and red sequence is 9.43×10^{-02}, and the KS of red sequence and blue cloud is 6.5×10^{-07}. The violin plots in the lower panel represent the same data as the cumulative histogram at the top.

is possibly an underestimate, as lenticular galaxies are often missed in visual inspections (Graham 2019).

3.3 Winding of spiral arms

Fig. 1, T05: *'How tightly wound do the spiral arms appear?'*

Green-valley galaxies tend to follow the blue cloud in behaviour in spiral arm windings of tight and medium, but lead in voting of loose winding. The red sequence continues to show the opposite behaviour to the blue cloud (see, for example, Figs 7, 8, and 9).

Since T05 is a choice between these three questions and one cannot progress without clicking one option, the plots in Figs 7, 8, and 9 are complementary. It shows that loose winding is preferred for the blue cloud and tight winding for the red sequence, and the green-valley voting behaviour is somewhere in between. It also shows that the 'medium' option voting is much more similar for all three populations as a compromise option, but remains less of a preference for red-sequence galaxies, strongly suggesting that red-sequence galaxies have tightly wound arms.

3.4 Number of spiral arms

Fig. 1, T06: *'How many spiral arms are there?'*

Green-valley galaxies are more symmetric (180° rotationally symmetric), as the higher relative voting fraction points out. They are favoured to have two arms, rather than one or three (which may be 120° symmetric). Spiral galaxies with an odd number of arms are more commonly found in the blue cloud, the voting suggests (see, for example, Fig. 10). The number of arms has been linked to specific star-formation decline (Porter-Temple et al. 2022) and the relative distributions of voting for three-armed spirals in the red sequence, green valley, and blue cloud reflect this.

3.5 Central bulge prominence

Fig. 1, T04: *'How prominent is the central bulge, compared with the rest of the galaxy?'*

Fig. 11 shows the voting behaviour for this question with the highest voting fractions, i.e. the largest fraction of the sample with high voting confidence, for a dominant bulge in the red sequence, followed by the green valley and blue cloud. This trend is an expected result following the current understanding of galaxy evolution from green valley to red sequence, i.e. discs fading and turning red and the bulge gaining relative prominence with respect to the disc.

3.6 Rings

Fig. 1, T10: *'Do you see any of these odd features in the image?'*

This last question in the question tree of GZ (Fig. 1) is for citizen scientists to identify rarer morphological phenomena, which are expected to be infrequent, such as accidental overlaps of galaxies along the line of sight (see Keel et al. 2013; Holwerda 2017, for a discussion on these). One of the options is to identify a ring, as opposed to a lensing object, as this odd feature.

Downloaded from https://academic.oup.com/mnras/article/517/3/4575/6795245 by Lancaster University user on 10 December 2022

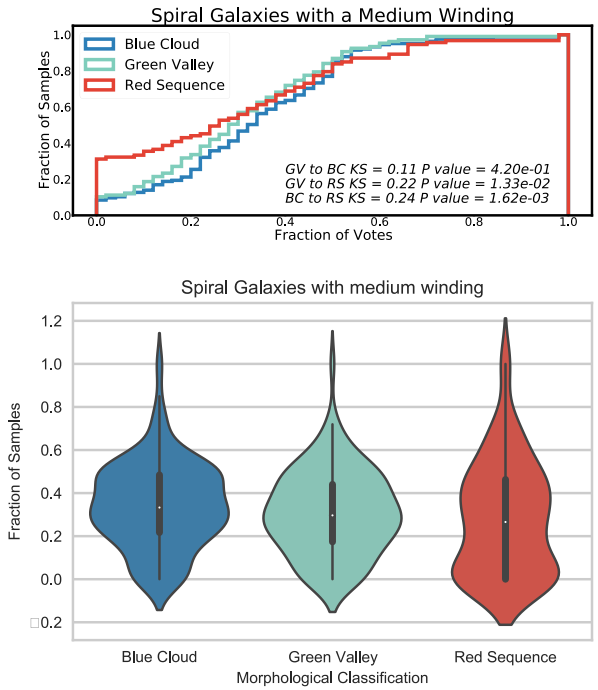

Figure 8. Histogram of the fraction of votes in favour of spiral galaxies having a medium winding (T05 in the GZ questionnaire). The difference between the green valley and blue cloud is distinguishable with a KS of 0.11, but the difference between the green valley and red sequence is distinguishable at a KS value of 0.22, and the largest difference is between the behaviour of the red sequence and the blue cloud with a KS of 0.24. The significances of these results are as follows: green valley to blue cloud has a p value of 4.2×10^{-01}, green valley to red sequence 1.33×10^{-02}, and blue cloud to red sequence 1.61×10^{-03}. This shows again how the behaviours of the blue cloud and red sequence are opposite, with the green valley maintaining the middle. The violin plots represent the same data as the cumulative histogram in the top panel.

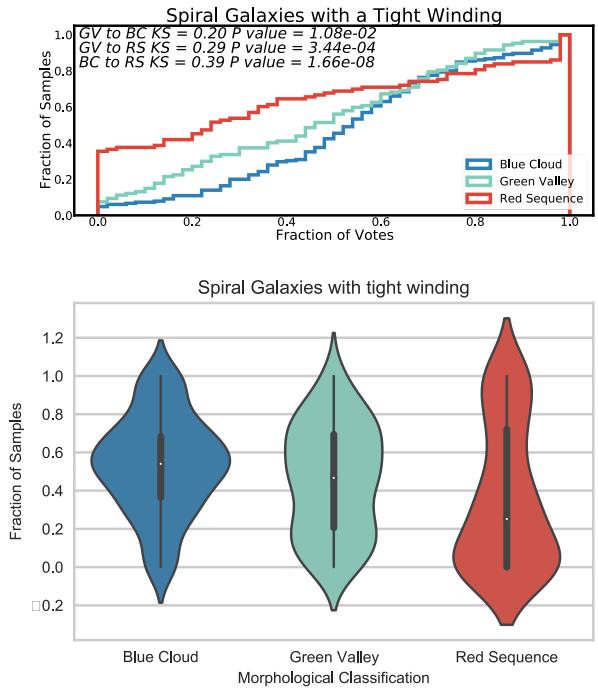

Figure 9. Histogram of the fraction of votes in favour of spiral galaxies having a tight winding (T05 in the GZ questionnaire). The difference between the green valley and blue cloud is distinguishable with a KS of 0.20, but the difference between the green valley and red sequence is 0.29, with the difference between the red sequence and blue cloud being the most distinguishable at 0.39. The significances of these are represented with p-values of the green valley and blue cloud of 1.08×10^{-02}, green valley and red sequence of 3.44×10^{-04}, and blue cloud and red sequence of 1.66×10^{-08}. The violin plots represent the same data as the top panel histograms.

Though the source of rings is still heavily debated, the abundance of inside quenching may be a potential cause (Kelvin et al. 2018). We expect a direct correlation between the presence of bars and rings in featured galaxies if the inside-out quenching theory holds true. We see this behaviour in the blue cloud and the red sequence (steady increase in bars in disc galaxies from blue cloud to red sequence, Fig. 5). However, there is an even stronger prevalence of ring galaxies in the green valley (Fig. 12). This could be a sign of increased inside quenching or ring formation in the green valley, driven by other possible factors.

4 DISCUSSION

The transition of galaxies from the star-forming blue cloud to the passive red sequence through the green valley is thought to be due to a variety of processes, both internal and external, and can be in either direction (see Salim 2014 for a review). There appears to be a relation between galaxy morphology and transition speed (Schawinski et al. 2014; Smethurst et al. 2015): smooth galaxies undergo a rapid transit through major mergers, intermediate complex galaxies (e.g. S0) undergo minor mergers and galaxy interactions for an intermediate crossing scale, and disc galaxies cross most slowly, due to secular processes. In disc galaxies, bars and bulges are suspected to play a role in the quenching process (Nogueira-Cavalcante et al. 2018; Ge et al. 2018; Gu et al. 2018; Kelvin et al. 2018). Green-valley quenching appears to be ongoing since $z \sim 2$ (Jian et al. 2020) with a mass dependence on transition speed and phase (Schawinski et al. 2014; Angthopo, Ferreras & Silk 2020). Higher mass galaxies appear to quench mostly due to lack of gas supply (Das, Pandey & Sarkar 2021) and quenching does seem linked to a lack of circumgalactic medium (CGM: Kacprzak et al. 2021). At lower masses, morphological features are thought to influence the quenching speed (Smethurst et al. 2015), motivating our morphological characterization of green-valley galaxies.

Citizen scientists were asked if the galaxies they were looking at were ring galaxies. We have analysed the GZ votes of galaxies of mass ($10.25 < \log(M_*/\mathrm{M}_\odot) < 10.75$), as was done in Kelvin et al. (2018). However, we increased the redshift from $z < 0.06$ to $z < 0.075$ thanks to the improved resolution of the KiDS images. This larger sample size gave us very similar overall results to those from Kelvin et al. (2018), i.e. a higher fraction of ring galaxies in green-valley featured galaxies. The data presented in Fig. 12 demonstrate this behaviour. Initially, we had constrained our sample to $z < 0.15$, the full redshift range of GAMA/GZ data. The results were qualitatively similar, but distance effects cannot be fully ruled out and we imposed the $z = 0.075$ limit (the distance KiDS resolution corresponds to a 1-kpc feature).

It is clear that the green valley has a higher concentration of ring-featured galaxies than both the red sequence and the blue cloud. This is not the only example of the green valley exhibiting its own behaviour: as explained in Section 3.3, the green valley has an initial

Downloaded from https://academic.oup.com/mnras/article/517/3/4575/6795245 by Lancaster University user on 10 December 2022

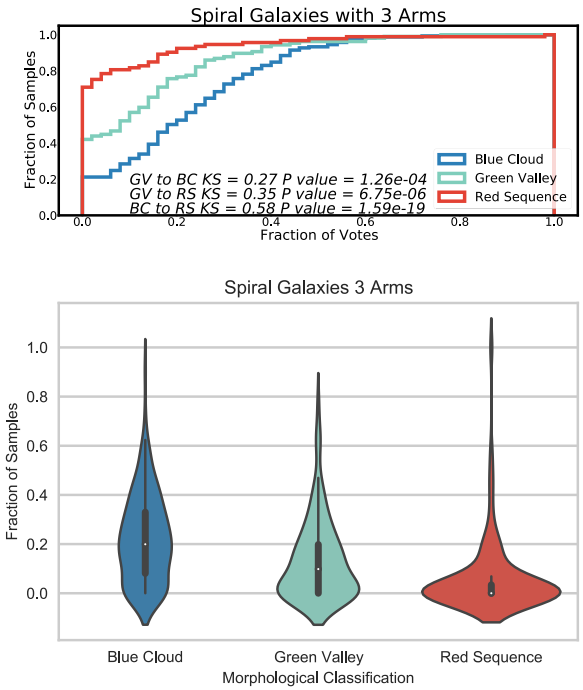

Figure 10. A histogram of the fraction of votes in favour of classifying galaxies as spiral with three arms (T10 in the GZ questionnaire). The difference between the green valley and blue cloud is very distinguishable with a K–S value of 0.27, green valley to red sequence is distinguishable with a K–S value of 0.35, and the highest difference is seen between blue cloud and red sequence with a K–S of 0.58. The significance from p-values is 1.26×10^{-04}, 6.75×10^{-06}, and 1.59×10^{-19}, respectively. This shows that spiral galaxies with three arms are found more frequently in the blue cloud and green valley. The violin plots represent the same data.

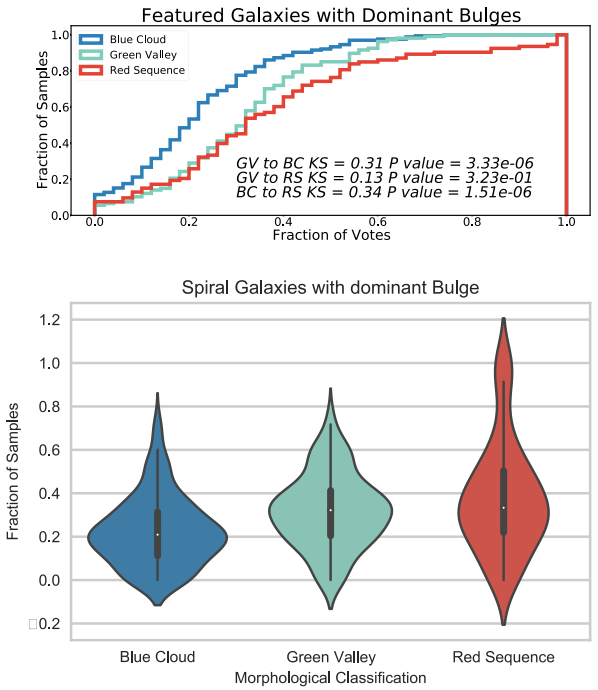

Figure 11. A histogram of the fraction of votes classifying disc galaxies with dominant bulges (T04 in the GZ questionnaire). The difference between the green valley and blue cloud is distinguishable with a K–S of 0.31. This difference is less distinguishable between the green valley and the red sequence, with a K–S value of 0.13. When comparing the blue cloud with the red sequence, the K–S value is 0.34. The significance p-values are 3.33×10^{-06}, 3.23×10^{-01}, and 7.55×10^{-03}, respectively.

behaviour of looser arm windings (Fig. 7). We have also shown that the red sequence and green valley have higher concentrations of featured galaxies with bars, while the blue cloud possesses the lowest amount of featured galaxies with bars (Fig. 5). Earlier studies found that barred galaxies may transition more slowly (Nogueira-Cavalcante et al. 2018), or that bulges play a role in the transition through the green valley (Ge et al. 2018), some of which may be rejuvenating rather than quenching (Mancini et al. 2019).

As previously stated, it is theorized that quenching may cause ring formation. The existence of bars may expedite the quenching process, which may in turn lead to faster ring formation. This shows a possible link between the role of bars and rings in galaxy quenching. The green valley represented in the histogram in Fig. 5 shows a difference in behaviour from that seen with rings in Fig. 12. The voting for bars in green-valley galaxies in Fig. 5 is in between the voting for the blue cloud and red sequence. The voting in the green valley in Fig. 12 is more confident in rings than either the blue cloud or the red sequence; a larger fraction of the green-valley sample has a higher confidence in rings than either comparison sample.

However, by looking at our violin graphs portion of Fig. 12, we see that the distribution of the green-valley galaxy sample is spread over the whole range of possible values (galaxies with high and low confidence in a ring), while the blue-cloud galaxies are mostly clustered at low confidence in rings while the red-sequence galaxies resemble a high-confidence and low-confidence population. The green valley resembles the red sequence, but with higher voting fractions.

This could be due to the fact that this is a transition zone and the younger green-valley galaxies have yet to exhibit the bar or ring behaviours that may occur later in their lifetimes in the green valley, just before entering the red sequence. Future studies with even more GZ information will help probe the link between bar and ring formation and the green-valley population.

Furthermore, we studied the possibility of a correlation between dominant bulges and rings (Figs 11 and 12, respectively). Though it does appear that the green valley is in the middle in both bulge and ring distributions, the role of internal quenching remains unclear. It is not clear why a fading disc will result in either a ring or a tightening of the spiral arm. Perhaps, over time, the reduction of gas in the disc results in a lower density for the spiral density wave (e.g. Roberts, Roberts & Shu 1975; Dobbs & Baba 2014; Shu 2016) and thus a different spiral pattern speed. This change in the spiral density wave could lead to either a tightening of the spiral arms or ring formation. This depends, however, on the dominant formation mechanism for spiral arms (Davis, Graham & Combes 2019). Rings could quench the disc or the quenching of the disc could form rings.

When all conditions are carefully considered, the preference for green-valley galaxies to be classified with rings suggests that any quenching in the green valley is accompanied by subtle changes in disc morphology, as well as mere dimming of the disc.

5 CONCLUSIONS

We find that the red sequence leads in the highest concentration of featured galaxies with bulges. It is followed by the green valley (Fig. 11). A lack of new-forming stars in the red sequence leads to a

Downloaded from https://academic.oup.com/mnras/article/517/3/4575/6795245 by Lancaster University user on 10 December 2022

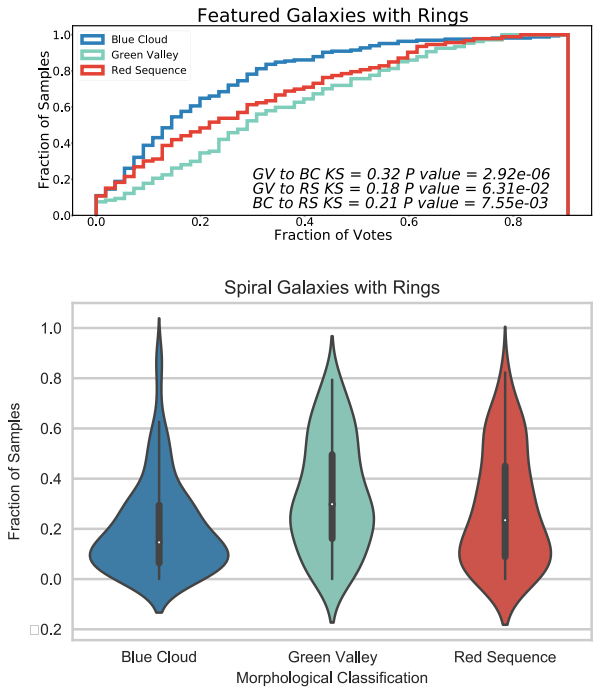

Figure 12. A histogram of the fraction of votes labelling galaxies as featured with rings (T06 in the GZ questionnaire). The green valley is distinguishable from the blue cloud with a K–S value of 0.32. The green valley continues to differ from the red sequence with a K–S value of 0.18, while the red sequence to blue cloud difference has a K–S value of 0.21. The significance p-values are 2.92×10^{-06}, 6.31×10^{-02}, and 7.55×10^{-03}, respectively. This is the first time we observe a difference in the location of the green-valley data. Here, it is no longer in between the blue cloud and the red sequence, thus presenting behaviour of its own.

lack of contrast, which may allow bulges to be more visible. This is the diametrically opposite case to bulges in the blue cloud.

Our results match GZ voting (on KiDS images) in confirming that green-valley featured galaxies have the most rings in comparison with their blue-cloud and red-sequence counterparts (Fig. 12). This confirms the initial prominence of rings in green-valley galaxies found by Kelvin et al. (2018).

Our findings also show a gradual loosening of spiral arms as galaxies enter the green valley. Blue-cloud galaxies are viewed predominantly with tightly wound arms, while every kind of spiral arm winding is present in the red sequence. A trend is visible in the voting on central bulge prominence: bulges become more dominant from blue cloud to red sequence, with the green valley displaying an intermediate distribution.

Our thorough study of galaxies classified in the green valley indicates that their behaviours typically share characteristics with both the red sequence and blue cloud, placing them in the middle (Fig. 6), thereby highlighting the transitional interstitial nature of the green valley.

ACKNOWLEDGEMENTS

This material is supported by NASA Kentucky award No. 80NSSC20M0047 (NASA-REU to LH and DS). DS thanks C. Nasr for her assistance.

This publication has been made possible by the participation of all the volunteers in the Galaxy Zoo project. Their contributions are individually acknowledged at http://www. Galaxy Zoo.org/Volunteers.aspx.

DATA AVAILABILITY

This work is predominantly based on public data from the GAMA survey (available at http://www.gama-survey.org/dr3/) and the Galaxy Zoo catalogue for the GAMA fields, to be released with DR4 (Driver et al. 2022).

REFERENCES

Angthopo J., Ferreras I., Silk J., 2020, MNRAS, 495, 2720
Arnouts S. et al., 2007, A&A, 476, 137
Baldry I. K., Glazebrook K., Brinkmann J., Ivezić Ž., Lupton R. H., Nichol R. C., Szalay A. S., 2004, ApJ, 600, 681
Baldry I. K., Balogh M. L., Bower R. G., Glazebrook K., Nichol R. C., Bamford S. P., Budavari T., 2006, MNRAS, 373, 469
Ball N. M., Loveday J., Brunner R. J., 2008, MNRAS, 383, 907
Bamford S. P. et al., 2009, MNRAS, 393, 1324
Barone T. M. et al., 2022, MNRAS, 512, 3828
Bell E. F. et al., 2004, ApJ, 600, L11
Bluck A. F. L. et al., 2020, MNRAS, 499, 230
Brammer G. B. et al., 2009, ApJ, 706, L173
Bremer M. N. et al., 2018, MNRAS, 476, 12
Coenda V., Martínez H. J., Muriel H., 2018, MNRAS, 473, 5617
Corcho-Caballero P., Ascasibar Y., López-Sánchez Á. R., 2020, MNRAS, 499, 573
Corcho-Caballero P., Casado J., Ascasibar Y., García-Benito R., 2021, MNRAS, 507, 5477
da Cunha E., Charlot S., Elbaz D., 2008, MNRAS, 388, 1595
Das A., Pandey B., Sarkar S., 2021, J. Cosmol. Astropart. Phys., 2021, 045
Davis B. L., Graham A. W., Combes F., 2019, ApJ, 877, 64
de Jong J. T. A., Verdoes Kleijn G. A., Kuijken K. H., Valentijn E. A., 2013, Exp. Astron., 35, 25
de Jong J. T. A. et al., 2015, A&A, 582, A62
de Jong J. T. A. et al., 2017, A&A, 604, A134
Dobbs C., Baba J., 2014, PASA, 31, e035
Driver S. P. et al., 2006, MNRAS, 368, 414
Driver S. P. et al., 2009, Astron. Geophys., 50, 5.12
Driver S. P. et al., 2011, MNRAS, 413, 971
Driver S. P. et al., 2016, ApJ, 827, 108
Driver S. P. et al., 2022, MNRAS, 513, 439
Faber S. M. et al., 2007, ApJ, 665, 265
Fraser-McKelvie A. et al., 2019, MNRAS, 488, L6
Fraser-McKelvie A. et al., 2020a, MNRAS, 495, 4158
Fraser-McKelvie A. et al., 2020b, MNRAS, 499, 1116
Ge X., Gu Q.-S., Chen Y.-Y., Ding N., 2018, preprint (arXiv:1808.01709)
Graham A. W., 2013, in Seigar M.S., Treuthardt P., eds, ASP Conf. Ser. Vol. 480, Structure and Dynamics of Disk Galaxies. Astron. Soc. Pac., San Francisco, p. 185
Graham A. W., 2019, MNRAS, 487, 4995
Graham A. W., Dullo B. T., Savorgnan G. A. D., 2015, ApJ, 804, 32
Graham A. W., Janz J., Penny S. J., Chilingarian I. V., Ciambur B. C., Forbes D. A., Davies R. L., 2017, ApJ, 840, 68
Gu Y., Fang G., Yuan Q., Cai Z., Wang T., 2018, ApJ, 855, 10
Holwerda B. W. et al., 2019, AJ, 158, 103
Holwerda B., 2017, in Gil de Paz A. , Lee J. C., Knapen J. H., eds, Proc. IAU Symp. 321, Formation and Evolution of Galaxy Outskirts. Cambridge Univ. Press, Cambridge, p. 248
Hopkins A. M. et al., 2013, MNRAS, 430, 2047
Jian H.-Y. et al., 2020, ApJ, 894, 125
Kacprzak G. G., Nielsen N. M., Nateghi H., Churchill C. W., Pointon S. K., Nanayakkara T., Muzahid S., Charlton J. C., 2021, MNRAS, 500, 2289
Keel W. C., Manning A. M., Holwerda B. W., Mezzoprete M., Lintott C. J., Schawinski K., Gay P., Masters K. L., 2013, PASP, 125, 2
Kelvin L. S. et al., 2018, MNRAS, 477, 4116

Downloaded from https://academic.oup.com/mnras/article/517/3/4575/6795245 by Lancaster University user on 10 December 2022

Kuijken K. et al., 2019, A&A, 625, A2
Lintott C. J. et al., 2008, MNRAS, 389, 1179
Liske J. et al., 2015, MNRAS, 452, 2087
Mancini C. et al., 2019, MNRAS, 489, 1265
Martin D. C. et al., 2005, ApJ, 619, L1
Martin D. C. et al., 2007, ApJS, 173, 342
Masters K. L. et al., 2010, MNRAS, 404, 792
Masters K. L. et al., 2021, MNRAS, 507, 3923
Mendez A. J., Coil A. L., Lotz J., Salim S., Moustakas J., Simard L., 2011, ApJ, 736, 110
Noeske K. G. et al., 2007, ApJ, 660, L43
Nogueira-Cavalcante J. P., Gonçalves T. S., Menéndez-Delmestre K., Sheth K., 2018, MNRAS, 473, 1346
Pan Y. C., Sullivan M., Maguire K., Gal-Yam A., Hook I. M., Howell D. A., Nugent P. E., Mazzali P. A., 2015, MNRAS, 446, 354
Peng C. Y., Ho L. C., Impey C. D., Rix H., 2010, AJ, 139, 2097
Phillipps S. et al., 2019, MNRAS, 485, 5559
Porter-Temple R. et al., 2022, MNRAS, 515, 3875
Roberts W. W. J., Roberts M. S., Shu F. H., 1975, ApJ, 196, 381
Salim S., 2014, Serbian Astron. J., 189, 1
Salim S. et al., 2007, ApJS, 173, 267
Schawinski K., 2009, MNRAS, 397, 717
Schawinski K. et al., 2007, ApJS, 173, 512
Schawinski K. et al., 2014, MNRAS, 440, 889
Shu F. H., 2016, ARA&A, 54, 667
Skibba R. A. et al., 2009, MNRAS, 399, 966
Smethurst R. J. et al., 2015, MNRAS, 450, 435
Smethurst R. J., Lintott C. J., Bamford S. P., Hart R. E., Kruk S. J., Masters K. L., Nichol R. C., Simmons B. D., 2017, MNRAS, 469, 3670
Strateva I. et al., 2001, AJ, 122, 1861
Taylor E. N. et al., 2011, MNRAS, 418, 1587
Taylor E. N. et al., 2015, MNRAS, 446, 2144
Willett K. W. et al., 2013, MNRAS, 435, 2835
Willmer C. N. A. et al., 2006, ApJ, 647, 853
Wright A. H. et al., 2017, MNRAS, 470, 283

APPENDIX A: SUPPLEMENTAL FIGURES

In this section we supply the histograms representing the rest of the GAMA questions that were not in the main text.

Table A1. Kolmogorov-Smirnov values in the GalaxyZoo voting distributions compared between different galaxy populations based on colour, red, green, and blue.

	KS values for histograms		
Figure	Green valley to blue cloud	Green valley to red sequence	Blue cloud to red sequence
5: Bars	0.16	0.10	0.24
6: Spiral	0.32	0.20	0.50
7: Loose	0.23	0.17	0.35
8: Medium	0.11	0.22	0.24
9: Tight	0.20	0.29	0.39
10: Three arms	0.27	0.35	0.58
11: Dominant bulge	0.31	0.13	0.34
12: Rings	0.32	0.18	0.21
A1: One arm	0.11	0.11	0.10
A2: Two arms	0.24	0.33	0.44
A3: Four arms	0.21	0.16	0.37
A4: Four+ arms	0.14	0.19	0.32
A5: Dust lane	0.07	0.15	0.17
A6: Mergers	0.10	0.21	0.13
A7: Lenses or arcs	0.14	0.14	0.07
A8: Tidal debris	0.18	0.14	0.24
A9: Obvious bulges	0.36	0.26	0.18

Downloaded from https://academic.oup.com/mnras/article/517/3/4575/6795245 by Lancaster University user on 10 December 2022

Table A2. The p-values of the Kolmogorov-Smirnov tests between different galaxy populations identified by colour (red, green, and blue).

Figure	*p*-values for histograms		
	Green valley to blue cloud	Green valley to red sequence	Blue cloud to red sequence
5: Bars	6.14×10^{-02}	6.22×10^{-01}	1.25×10^{-03}
6: Spiral	1.39×10^{-06}	3.12×10^{-02}	5.66×10^{-14}
7: Loose	2.16×10^{-03}	9.43×10^{-02}	6.50×10^{-07}
8: Medium	4.20×10^{-01}	1.33×10^{-02}	1.62×10^{-03}
9: Tight	1.08×10^{-02}	3.44×10^{-04}	1.66×10^{-08}
10: Three arms	1.26×10^{-04}	6.75×10^{-06}	1.59×10^{-19}
11: Dominant bulge	3.33×10^{-06}	3.23×10^{-01}	1.51×10^{-06}
12: Rings	2.92×10^{-06}	6.31×10^{-02}	7.55×10^{-03}
A1: One arm	3.67×10^{-01}	5.17×10^{-01}	5.93×10^{-01}
A2: Two arms	8.62×10^{-04}	2.27×10^{-05}	4.97×10^{-11}
A3: Four arms	6.77×10^{-03}	1.23×10^{-01}	9.97×10^{-08}
A4: Four+ arms	1.22×10^{-01}	5.23×10^{-02}	7.57×10^{-06}
A5: Dust lane	9.07×10^{-01}	2.15×10^{-01}	4.62×10^{-02}
A6: Mergers	5.34×10^{-01}	1.81×10^{-02}	2.70×10^{-01}
A7: Lenses or arcs	1.54×10^{-01}	2.76×10^{-01}	8.63×10^{-01}
A8: Tidal debris	1.54×10^{-01}	5.64×10^{-02}	1.75×10^{-03}
A9: Obvious bulges	2.19×10^{-04}	5.68×10^{-02}	3.12×10^{-07}

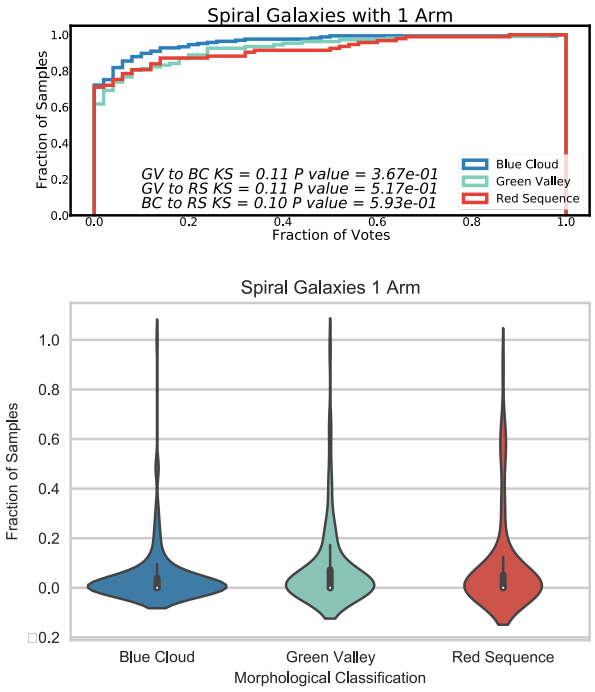

Figure A1. Histogram of the fraction of votes in favour of galaxies having one arm (T10 in the GZ questionnaire). The difference between the green valley and blue cloud is not very distinguishable with a KS of 0.06; the green valley is more distinguishable from the red sequence with a KS value of 0.12, keeping the green valley between the behaviour of the red sequence and blue cloud, which has the most difference with a KS value of 0.18. The significance between the green valley and blue cloud is 0.1, green valley and red sequence 4.18×10^{-05}, and blue cloud and red sequence 5.48×10^{-11}.

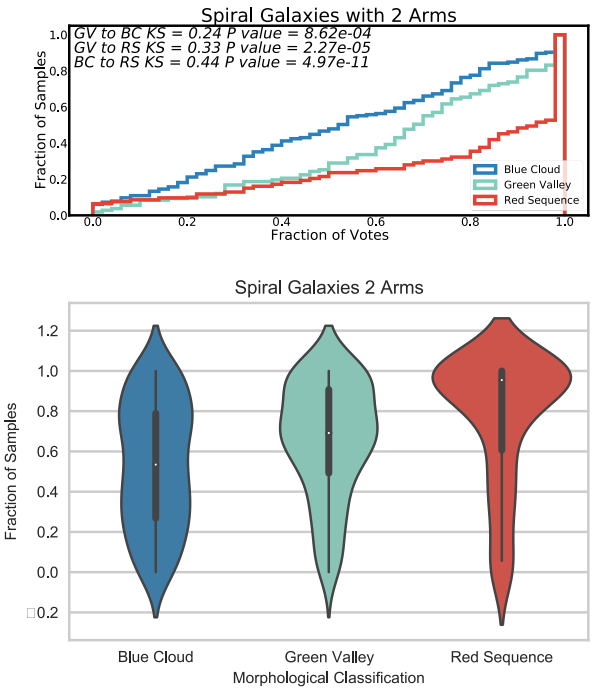

Figure A2. Histogram of the fraction of votes in favour of galaxies having two arms (T10 in the GZ questionnaire). The difference between the green valley and blue cloud is distinguishable with a KS of 0.18, while the green valley is distinguishable from the red sequence with a KS value of 0.17, staying between the behaviour of the blue cloud and red sequence with a KS of 0.33. The significance between the green valley and blue cloud is 1.14×10^{-10}, green valley and red sequence 1.93×10^{-09}, and blue cloud and red sequence 4.89×10^{-34}.

Downloaded from https://academic.oup.com/mnras/article/517/3/4575/6795245 by Lancaster University user on 10 December 2022

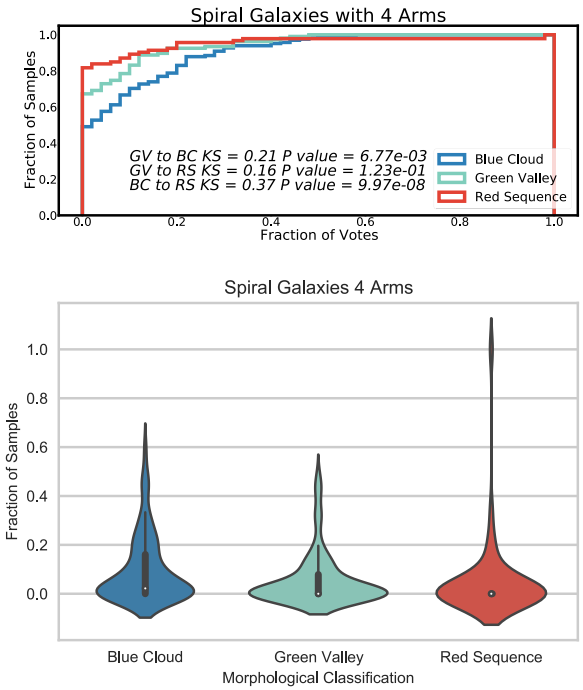

Figure A3. Histogram of the fraction of votes in favour of galaxies having four arms (T10 in the GZ questionnaire). The difference between the green valley and blue cloud is distinguishable with a KS of 0.17, while the green valley is less distinguishable from the red sequence with a KS value of 0.06, staying between the behaviour of the blue cloud and red sequence with a KS of 0.22. The significance between the green valley and blue cloud is 5.32×10^{-09}, green valley and red sequence 0.15, and blue cloud and red sequence 3.5×10^{-16}.

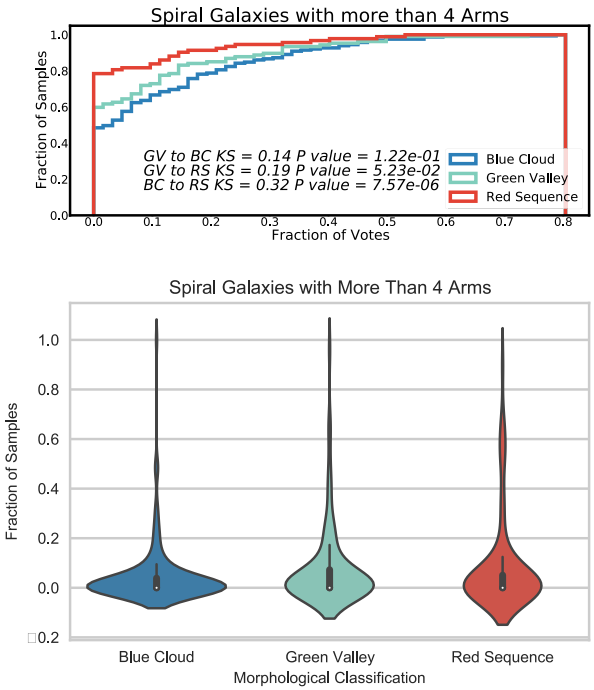

Figure A4. Histogram of the fraction of votes in favour of galaxies having more than four arms (T10 in the GZ questionnaire). The difference between the green valley and blue cloud is distinguishable with a KS of 0.14, the green valley is less distinguishable from the red sequence with a KS value of 0.06, and the KS of the blue cloud and red sequence is 0.20. The significance between the green valley and blue cloud is 3.12×10^{-06}, green valley and red sequence 0.1, and blue cloud and red sequence 7.81×10^{-13}.

Downloaded from https://academic.oup.com/mnras/article/517/3/4575/6795245 by Lancaster University user on 10 December 2022

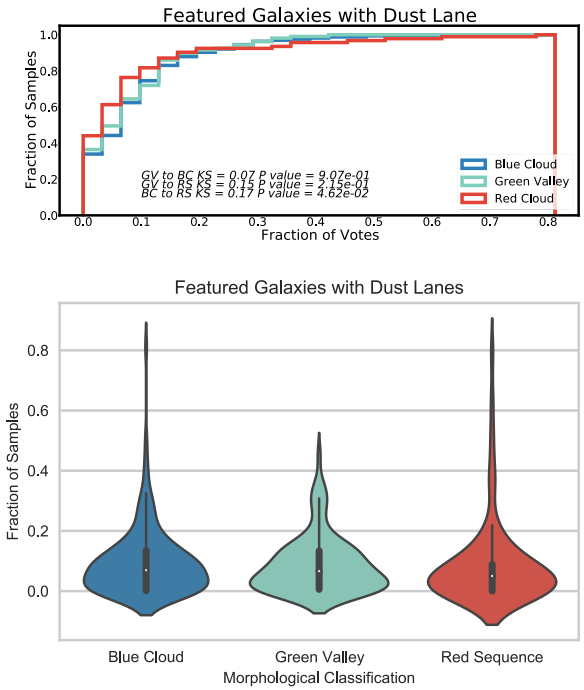

Figure A5. Histogram of the fraction of votes in favour of galaxies having dust lanes (T06 in the GZ questionnaire). The green valley is distinguishable from the blue cloud and red sequence with a KS value of 0.08 for both, while the red sequence and blue cloud are distinguishable with a KS value of 0.13. The significance between the green valley and blue cloud is 0.02, green valley and red sequence 0.02, and blue cloud and red sequence 5.36×10^{-06}.

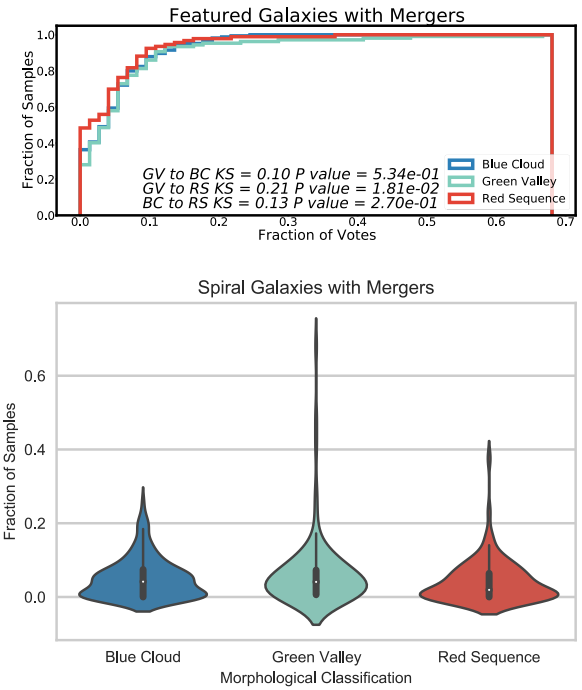

Figure A6. Histogram of the fraction of votes in favour of galaxies having mergers (T05 in the GZ questionnaire). The green valley is distinguishable from the blue cloud with a KS value of 0.09, the green valley continues to be differentiated from the red sequence with a KS value of 0.12, while the red sequence and blue cloud have a KS value of 0.18. The significance between the green valley and blue cloud is 8.05×10^{-03}, green valley and red sequence 6.8×10^{-05}, and blue cloud and red sequence 3.78×10^{-11}.

Downloaded from https://academic.oup.com/mnras/article/517/3/4575/6795245 by Lancaster University user on 10 December 2022

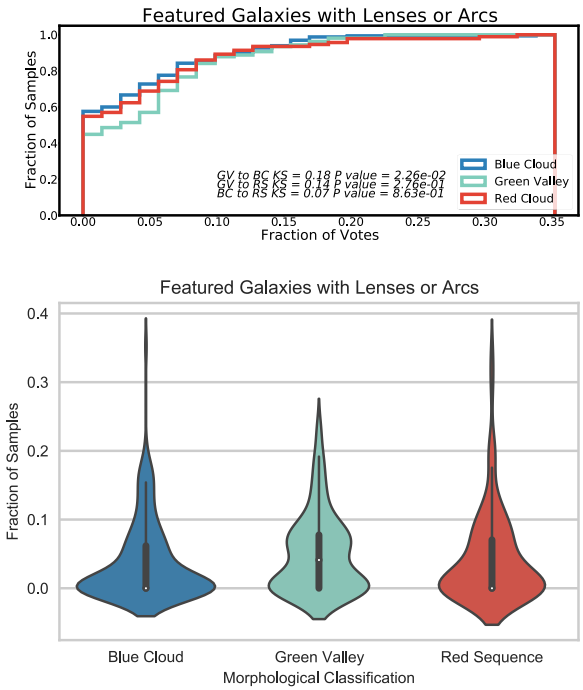

Figure A7. Histogram of the fraction of votes in favour of galaxies having lenses or arcs (T06 in the GZ questionnaire). The green valley to blue cloud KS value is 0.04, the green valley to red sequence KS is 0.10, and the red sequence to blue cloud has a KS value of 0.09. The significance between the green valley and blue cloud is 0.4, green valley and red sequence 1.81×10^{-03}, and blue cloud and red sequence 6.74×10^{-03}.

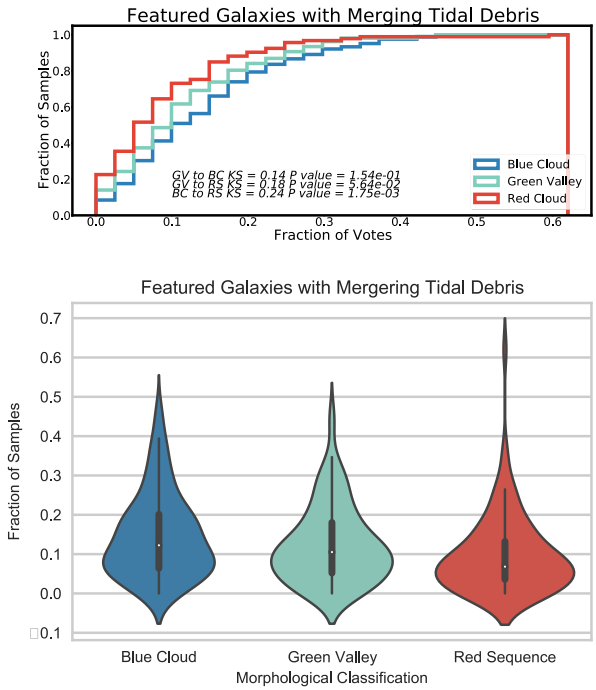

Figure A8. Histogram of the fraction of votes in favour of galaxies having tidal debris (T05 in the GZ questionnaire). The green valley is distinguishable from the blue cloud with a KS value of 0.19, the green valley continues to be differentiated from the red sequence with a KS value of 0.19, while the red sequence and blue cloud have a KS value of 0.35. The significance between the green valley and blue cloud is 1.78×10^{-11}, green valley and red sequence 5.63×10^{-12}, and blue cloud and red sequence 3.30×10^{-39}.

Downloaded from https://academic.oup.com/mnras/article/517/3/4575/6795245 by Lancaster University user on 10 December 2022

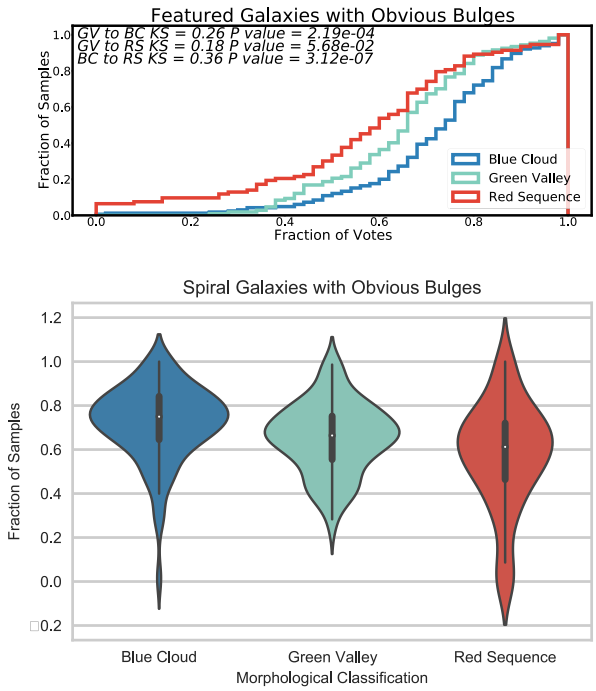

Figure A9. Histogram of the fraction of votes in favour of galaxies having obvious bulges (T04 in the GZ questionnaire). The difference between the green valley and blue cloud is distinguishable with a KS of 0.21, while the green valley is less distinguishable from the red sequence with a KS value of 0.11, staying between the behaviour of the blue cloud and red sequence, which have a KS of 0.25. The significance between the green valley and blue cloud is 6.64×10^{-14}, green valley and red sequence 6.5×10^{-04}, and blue cloud and red sequence 3.66×10^{-20}.

This paper has been typeset from a TEX/LATEX file prepared by the author.

Downloaded from https://academic.oup.com/mnras/article/517/3/4575/6795245 by Lancaster University user on 10 December 2022